Linearized Regge calculus and the J-Cost objective on an augmented simplicial ledger

Jonathan Washburn[1] and Philip Beltracchi[1]

[1]Recognition Physics Institute, Austin, Texas, USA ,
jon@recognitionphysics.org, pbeltracchi@recognitionphysics.org

May 2026

Abstract

Previously published Recognition Science work on gravity involved scale dependent source side enhancement to the Poisson equation in Newtonian gravity. In this paper, we examine a simplified model showing how something like a geometric gravity could arise from Recognition Science concepts. Specifically, we show how the Recognition Science ledger, originally a graph isomorphic to a cubic lattice undergoing tick based discrete updates, can be endowed with additional structure (deformable edge lengths and flat space cell interiors) allowing for it to be used as a substrate for Regge calculus. We then show that given certain conditions on hinge data, the Regge action can be recast as a Dirichlet form in terms of a potential defined on the nodes. Finally, we speak about the connections of this geometric approach with the previous Poisson equation approach, and speculate on possible modifications and adaptations of the Poisson equation approach for future testing.

Contents

1 Introduction **2**

2 Recognition Science preliminaries **4**
2.1 The Recognition Composition law 4
2.2 The Original Ledger 5
2.3 Constants from φ 5

3 Brief introduction to Regge calculus **6**
3.1 Riemann Tensor and Ricci scalar 7
3.1.1 Multiple joints and the Bianchi identities for 3D Euclidean manifolds 7
3.2 4D Lorentzian manifolds, generalized Hilbert action, and field equations . 9
3.2.1 Sketch of the proof $\sum_n L_n \frac{\partial \epsilon_n}{\partial l_p} = 0$ 10
3.3 Weak field Regge action 11

4 The Ledger as a Regge calculus substrate **12**
4.1 Ledger cost 14

5 The Field-Curvature relationship **14**
5.1 The Regge action with the conformal edge length ansatz 14
5.1.1 Emergence of the Dirichlet form 15
5.1.2 Reduction of the action: What has been proven 15
5.1.3 Reduction of the action: What has not been proven 16
5.2 The Weak Field Identification 16
5.2.1 Lean modules for formal verification 17

6 Toward recovery of General Relativity from Regge calculus **19**
6.1 Advantages of the RS Cubic Lattice in a hypothetical GR recovery . . . 19
6.2 Possible difficulties with the RS Cubic Lattice 20
6.3 The strong field regime 21

7 Discussion **21**
7.1 Connection to the ILG work 21
7.2 Relation to Other Regge Calculus Approaches 22

8 Conclusion **23**

A Geometry of tetrahedra **23**
A.1 The single tetrahedron Schläfli 24
A.2 A Freudenthal tetrahedron 25

B Standard Linearized General Relativity **25**
B.1 Emergence of the Poisson equation 27

C Information-Limited Gravity: Detailed analysis and essential modifications **28**
C.1 relation between published t and k forms of ρ_{eff} 28
C.2 Motivating the surrogate 28
C.3 Problems with the forms of (58) and (59) 29
C.4 Possible modifications to the ILG kernels and future work 30

1 Introduction

General relativity represents gravity geometrically, through spacetime curvature. The Einstein field equations

$$G_{\mu\nu} + \Lambda\, g_{\mu\nu} = \kappa\, T_{\mu\nu} \tag{1}$$

relate the geometry of spacetime (via the Einstein tensor $G_{\mu\nu}$) to its matter content (via the stress-energy tensor $T_{\mu\nu}$), with $\kappa = 8\pi G/c^4$ as the gravitational coupling constant.

Modern physics typically treats field equations as being derived from stationary action under variation of the underlying field. In the case of GR, the action decomposes as

$$S = \int (\frac{R - 2\Lambda}{2\kappa} + L_M)\sqrt{-g}d^4x \tag{2}$$

where the variation is conventionally taken over the inverse metric, or sometimes both the inverse metric and the connection (see e.g. [1] for a textbook presentation). Here

R is the Ricci scalar, Λ is a cosmological constant, L_M is a matter Lagrangian density whose variation leads to $T_{\mu\nu}$, and $-g$ is the negative of the metric determinant.

There are some pleasing attributes to this:

1. Constructing gravity as a geometric effect makes equivalence of inertial and gravitational mass automatic.

2. The geometric portion of the action consists of a constant Λ and the unique independent lowest order scalar in terms of metric derivatives, which are arguably the simplest possible terms.

3. A version of energy and momentum conservation, $\nabla_\mu T^\mu_\nu = 0$, is guaranteed by the geometric Bianchi identities and field equation.

4. Empirically, General Relativity has been greatly successful in all precision tests with controlled experiments such as deviations from Newtonian gravity in the weak field, gravitational time dilation, and frame dragging. More recently, experiments have been able to constrain gravitational wave emission and propagation, and strong field behavior near neutron stars and black holes. See [2, 3, 4] for review articles on these topics.

However, there are a few outstanding problems:

1. Beyond its role in inducing the energy momentum tensor, L_M is unspecified. The anomalies on galactic and larger scales could be explained either by new gravitational effects or additional matter sources.

2. GR seems to predict the emergence of situations where curvature singularities form and its own geometric picture is invalid [5, 6].

3. Despite enormous effort, there is no widely accepted way to make general relativity and quantum mechanics compatible. See [7, 8, 9] for recent review articles.

4. The values for the constants κ and Λ are parameters that must be measured, and have values that are widely considered to be oddly small compared to hypothetical identifications. The observed Λ, compared to naively considering vacuum quantum fluctuations, is sometimes cited as a factor 10^{120}[1] or 10^{122} [10] too small, although more sophisticated calculations bring the factor to "only" 10^{54} [10]. The value for κ is not dimensionless so it is difficult to make a direct comparison to the QFT coupling constants, but gravity is considered to be $10^{30} - 10^{40}$ times weaker.

5. It is somewhat surprising that the spacetime background matter inhabits reacts to the matter at all.

There are of course various programs attempting to rectify these issues. One relatively new program is Recognition Science. Starting from a single functional equation — the Recognition Composition Law — RS derives a unique cost function, and then shows how the golden ratio, three spatial dimensions, the 8-tick period, and fundamental constants emerge [11].

There has been a previous paper dealing with gravitational physics in the Recognition Science framework, where they examined modifications to the source side of Poisson's equation in the context of galactic rotation curves. We give a brief summary of this

paper in Section 7.1 and perform detailed analysis and speculate on possible extensions to that approach in Appendix C, but stress that their Poisson equation modifications fundamentally treat gravity in terms of classical forces and accelerations.

This paper differs by examining a simplified system for how a geometric gravity might arise in the Recognition Science framework. Specifically, the canonical Recognition Science ledger is extended to have additional properties, after which it can be treated as a substrate for the Regge calculus [12] (see [13, 14] for reviews). We need to be clear from the outset: that the procedure as outlined in this paper, while related to geometric gravity, does not fully recover general relativity. The full set of relevant geometries in general relativity involve deformations beyond what is considered here.

2 Recognition Science preliminaries

2.1 The Recognition Composition law

The Recognition Composition Law (RCL) states that the recognition cost for positive ratio comparisons, when two comparisons are done, obeys

Definition 2.1 (Recognition Composition Law)**.**

$$\boxed{\mathrm{J}(xy) + \mathrm{J}(x/y) = 2\ \mathrm{J}(x)\ \mathrm{J}(y) + 2\ \mathrm{J}(x) + 2\ \mathrm{J}(y)} \tag{3}$$

This is a calibrated form of the d'Alembert functional equation. The RCL is not an arbitrary choice: from the class of more general polynomials $P(J(x), J(y))$ of degree 2 or less for the right hand side, normalization $J(1) = 0$ implies $P(J(x), J(y)) = 2J(x) + 2J(y) + cJ(x)J(y)$ for some constant c[15]. However, for all $c \neq 0$[1] the solutions are related by a coordinate rescaling, so choosing a value is essentially choosing a coordinate scale rather than a qualitatively different solution type [15].

Theorem 2.2 (Cost Uniqueness — T5)**.** *The unique solution [11] to* (3) *under calibration* $\lim_{t\to 0} 2J(e^t)/t^2 = 1$ *is*

$$\mathrm{J}(x) = \frac{1}{2}\big(x + x^{-1}\big) - 1 = \frac{(x-1)^2}{2x}, \qquad x > 0. \tag{4}$$

Key properties:

- $\mathrm{J}(x) \geq 0$ with equality iff $x = 1$ (identity has zero cost).
- $\mathrm{J}(x) = \mathrm{J}(x^{-1})$ (reciprocal symmetry).
- J is strictly convex on $(0, \infty)$ with $\mathrm{J}''(x) = x^{-3}$.
- In log coordinates: $\mathrm{J}(e^u) = \cosh(u) - 1$.

The argument x is typically a ratio of two things being compared. If there are events E_1 and E_2 and a positive scale map [16] from the event space [17] to the positive reals $\iota : E \to \mathbb{R}_{>0}$, then

$$x = \frac{\iota(E_1)}{\iota(E_2)} \tag{5}$$

[1] Using $c = 0$ *does* give something qualitatively different, $J(x) = k(\ln(x))^2$ [15].

2.2 The Original Ledger

The original presentation of the ledger in a publication [18] focused on costed comparisons and discrete dynamics of functions defined on nodes of graphs isomorphic to hypercubic lattices. The minimal period under which a cycle can run through D spatial dimensions on a hypercube is 2^D, and topological linking of cycles isolates $D = 3$, and hence $2^D = 8$, as canonical choices.

A minimal extension to this version of the ledger, important for applications to physics, is the addition of a uniform edge length l_0. For a positive real function $\psi(X)$ defined on the elements X, the total cost of nearest neighbor comparison on the lattice will be

$$J_{NN} = \sum_X \sum_{\hat{i}} J(\psi(X)/\psi(X + \hat{i})) + J(\psi(X)/\psi(X - \hat{i})), \tag{6}$$

where $\hat{i}$ ranges over the unit vectors. Using $\xi(X) = \log(\psi(X))$, it is possible to show that if the nearest neighbor terms are sufficiently similar and ℓ_0 is sufficiently small, then

$$\frac{\delta(J_{NN}/\ell_0^2)}{\delta\xi(X_0)} = 0 \Rightarrow \nabla^2\xi = 0. \tag{7}$$

More complex objectives, such as also comparing to the value at the previous time tick, allow for systems that mimic standard PDEs under the appropriate circumstances.

2.3 Constants from φ

The golden ratio $\varphi = \frac{1+\sqrt{5}}{2}$ is the unique positive root to the self- similarity equation $x^2 = x + 1$. It is considered to be of fundamental importance in the construction of constants of nature in RS.

The conventional ledger spacing is

$$\ell_0 = \lambda_{rec} = \sqrt{\pi G\hbar/c^3} \approx 2.86 \cdot 10^{-35} m \tag{8}$$

Adopting units where $c = \ell_0 = 1$, we have

$$\pi G\hbar = 1. \tag{9}$$

Another defined unit is the fundamental energy quantity

$$E_{\mathrm{f}} = \frac{c\hbar}{\ell_0} \approx 1.10 \cdot 10^9 J \tag{10}$$

as the value

$$E_{\mathrm{f}} = \varphi^{-k} \tag{11}$$

where $k = 2^D - D = 5$ for $D = 3$. Therefore, under the RS canonical units, we have

$$c = 1, \ell_0 = 1, E_{\mathrm{f}} = \hbar = \varphi^{-5}, G = \frac{\varphi^5}{\pi}, \kappa = 8\varphi^5 \tag{12}$$

In the RS canonical units, the following identities are consequences:

- $G\hbar = \varphi^5/\pi \cdot \varphi^{-5} = 1/\pi$ (Planck area $= 1/\pi$ in RS units).
- $\kappa\hbar = 8\varphi^5 \cdot \varphi^{-5} = 8$ (8-tick cadence from $2^D = 8$).
- $\pi G\hbar = 1$ (geometry $\times$ gravity $\times$ quantum $= 1$).

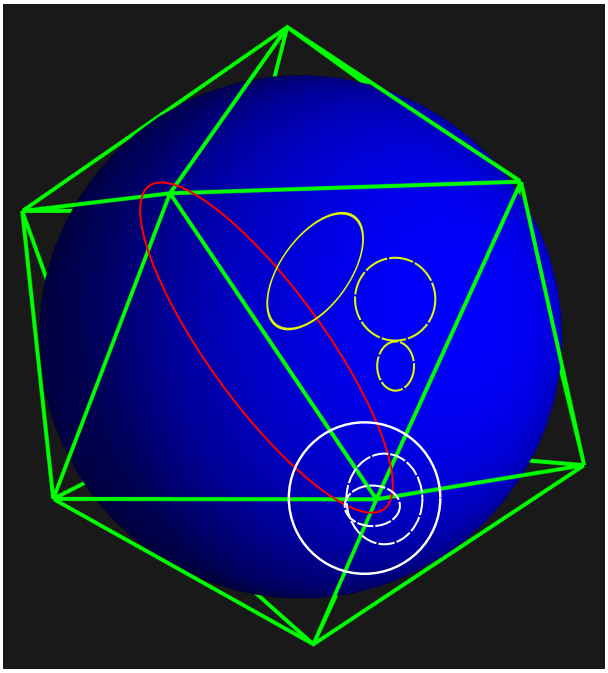

Figure 1: Approximation of a smooth manifold (sphere) with a triangulation, in this case an icosahedron. Less faithful analogues using fewer triangles (e.g. a tetrahedron or octahedron) or more faithful analogues with more triangles are possible. Loops on the triangulated manifold illustrated with the same color can be transformed into each other without encountering a vertex, so they share a holonomy class. Loops of the same color that are also dashed share the starting/ending point, so they share a homotopy class. The white loops enclose a deficit angle of $\pi/3$, the red loop $2\pi/3$, and the yellow loops 0.

3 Brief introduction to Regge calculus

In order to understand how a modified ledger can act as a substrate to Regge calculus, and what kind of modifications need to be made, it is prudent to explain what Regge calculus is and how it works. We mostly follow Regge's presentation from the original work [12], another helpful tutorial to Regge calculus is the preprint [19].

The basic idea behind the Regge calculus is the approximation of curved manifolds with flat simplices. Consider first approximating a 2D surface with triangles. Some set of n triangles will meet at a common vertex with angles $\theta_1, \theta_2, ...\theta_n$. If the surface is a flat plane, then $\sum_n \theta_n = 2\pi$. If the surface is curved, then $\sum_n \theta_n = 2\pi - \epsilon_v$, where ϵ_v is the deficit angle at that vertex. In terms of parallel transport around loops, a vector transported around a loop fully within a triangle will not rotate (the space within the triangle is flat), but a vector parallel transported around a loop containing a vertex will rotate by the vertex deficit angle, and loops containing multiple vertices will have the effects add. Therefore, the effective curvature can be considered as Dirac type distributions around the vertices. Loops that may be continuously deformed to each other without encountering the effective curvature Dirac distributions form an equivalence class (holonomy), and if they additionally share the same starting and ending point they form a more restrictive equivalence class (homotopy). An illustration showing the triangulated manifold and loop classes is in Figure 1.

3.1 Riemann Tensor and Ricci scalar

In higher dimensions N, the curvature is concentrated on $N-2$ dimensional simplices that Regge calls "bones", though the term "hinges" is also sometimes used (e.g. [20, 21]). For 3D Riemannian volume type manifolds, the bones will be line segments, and this is the situation in which Regge first formalizes the correspondence between the bones and the Riemann curvature tensor. The change in a vector A around a loop in smooth manifold differential geometry is

$$\delta A^{\mu} = \frac{1}{2} R_{\alpha\beta}{}^{\mu\gamma} \, {}^{*}\Sigma^{\alpha\beta} A_{\gamma} \tag{13}$$

where Σ is the area vector of the loop and ${}^{*}\Sigma^{\alpha\beta} = \varepsilon^{\alpha\beta\nu}\Sigma_{\nu}$ is its dual. Conversely, consider a bundle with density ρ of parallel bones, pointed along a unit vector U, each with deficit angle ϵ. If we are confined to a small approximately flat Euclidean patch, then the rotation angle of a parallel transported vector will be the number of bones through the loop times the deficit angle. The number of bones can be computed using the loop normal vector Σ and bone unit vector U

$$N = \rho \Sigma^{\mu} U_{\mu}. \tag{14}$$

and the change in the vector can be written as

$$\delta A^{\mu} = \rho \epsilon \Sigma^{\nu} U_{\nu} \varepsilon^{\mu\alpha\beta} U_{\alpha} A_{\beta}. \tag{15}$$

Defining a dual to the unit vector ${}^{*}U_{\alpha\beta} = \varepsilon_{\alpha\beta\gamma} U^{\gamma}$, this can be rewritten as

$$\delta A^{\mu} = \frac{1}{2} \rho \epsilon \, {}^{*}U_{\alpha\beta} \, {}^{*}U^{\mu\gamma} \, {}^{*}\Sigma^{\alpha\beta} A_{\gamma}. \tag{16}$$

Comparing (13) and (16), the evident identification for the effective curvature tensor in the discretized manifold is

$$R_{\alpha\beta}{}^{\mu\gamma} \Longleftrightarrow \rho \epsilon \, {}^{*}U_{\alpha\beta} \, {}^{*}U^{\mu\gamma} \tag{17}$$

. Because ${}^{*}U$ is the dual to a unit vector, this can be contracted easily to obtain the Ricci scalar

$$R \Longleftrightarrow 2\rho\epsilon. \tag{18}$$

While Regge [12] and the tutorial [19] derive the Riemann curvature tensor and vector parallel transport formulas as an explicitly 3D Euclidean situation, Regge claims that (18) is true in arbitrary dimension.

3.1.1 Multiple joints and the Bianchi identities for 3D Euclidean manifolds

Regge's next generalization involves considering we have m sets of parallel bones diverging from an identical set of joints, such that the simplex Riemann tensor becomes [12]

$$R_{\alpha\beta\gamma\mu} = \sum_{p=1}^{m} \rho_{(p)} \epsilon_{(p)} \, {}^{*}U^{(p)}_{\alpha\beta} \, {}^{*}U^{(p)}_{\gamma\mu}. \tag{19}$$

Let the joints have density[2] j. The number of bones in a bundle leaving a region will be the number entering the region plus the number leaving joints enclosed in the region,

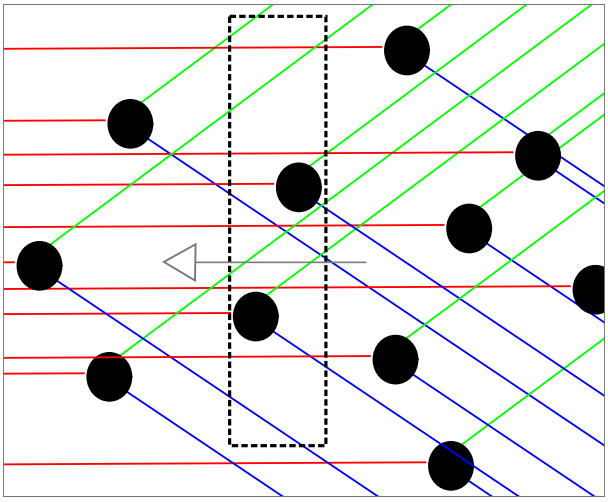

Figure 2: The red bones are parallel to the arrow (giving the vector $U_{(p)}$). 5 enter the right side of the box and 7 leave the left side because there are 2 joints inside the box.

see Figure 2 In the limit that the "box" is thin with height along the p^{th} bundle of bones ds and surface Σ. Then the density ρ_p of the p^{th} bundle obeys $\rho_p(s+ds) - \rho_p(s) = jds$, or $U^{\mu}_{(p)}\partial_\mu \rho_p = j$. Because there is no curvature away from the bones, the covariant derivatives reduce to partial derivatives and the Bianchi identities become

$$\partial_\nu R_{\gamma\mu\alpha\beta} + \partial_\gamma R_{\mu\nu\alpha\beta} + \partial_\mu R_{\nu\gamma\alpha\beta} = 0 \tag{20}$$

Because the joints are ostensibly identical, ϵ_p and $U_{(p)}$ are constant, so we obtain

$$0 = \partial_\nu \Big(\sum_{p=1}^{m} \rho_{(p)}\epsilon_{(p)} \ {}^*U^{(p)}_{\alpha\beta} \ {}^*U^{(p)}_{\gamma\mu} \Big) + \partial_\gamma \Big(\sum_{p=1}^{m} \rho_{(p)}\epsilon_{(p)} \ {}^*U^{(p)}_{\alpha\beta} \ {}^*U^{(p)}_{\mu\nu} \Big) + \partial_\mu \Big(\sum_{p=1}^{m} \rho_{(p)}\epsilon_{(p)} \ {}^*U^{(p)}_{\alpha\beta} \ {}^*U^{(p)}_{\nu\gamma} \Big) \tag{21}$$

$$0 = \sum_{p=1}^{m} \epsilon_{(p)} \ {}^*U^{(p)}_{\alpha\beta} \Big[\ {}^*U^{(p)}_{\gamma\mu}\partial_\nu(\rho_{(p)}) + \ {}^*U^{(p)}_{\mu\nu}\partial_\gamma(\rho_{(p)}) + \ {}^*U^{(p)}_{\nu\gamma}\partial_\mu(\rho_{(p)}) \Big] \tag{22}$$

[2]Confusingly, Regge also writes the joint density as ρ, we introduce the new notation here to avoid confusion with the bone density in the parallel case

which reduces [3] to

$$0 = j\varepsilon_{\nu\gamma\mu} \sum_{p=1}^{m} \epsilon_{(p)} \ {}^{*}U^{(p)}_{\alpha\beta} \tag{23}$$

3.2 4D Lorentzian manifolds, generalized Hilbert action, and field equations

There are subtleties in extending to a Lorentzian rather than Euclidean metric, as well as in moving to higher dimensions. Indeed, lower dimensional and Euclidean cases are frequently (see examples listed in the review article [14]) considered for simplicity, and aspects of 4D Lorentzian Regge calculus are not fully understood. Nevertheless, the bones are effectively triangular (2 simplexes) on the 4D Lorentzian manifold, and Regge defines a bone size parameter L through two sides A and B via

$$4L^2 = (A_\mu B^\mu)^2 - (A^\mu A_\mu)(B^\mu B_\mu). \tag{24}$$

The deficit angle is still defined through $2\pi - \sum_k \theta^k_n = \epsilon_n$ where θ^k_n is the dihedral angle of simplex k at bone n. Due to the metric signature Lorentzian angles may in theory be imaginary. Regge claims to consider bones with real deficit only, but work extending the Lorentzian Regge action directly in terms of complex variables exists [22, 23, 24].

The standard Hilbert term for the gravitational action is

$$\frac{1}{2\kappa} \int R\sqrt{-g} d^4x \tag{25}$$

Recall now a few ingredients:

1. The effective Ricci scalar in the parallel bone bundle case is $2\rho\epsilon$.
2. $\sqrt{-g}$ and bone size L are effectively size parameters.
3. The integral will go to a sum.

Regge proposes that the action can be written as a sum over the bones

$$S_{\text{Regge}} = \frac{1}{\kappa} \sum_n L_n \epsilon_n \tag{26}$$

[3] Specifically, the term in square brackets in (22) reduces with manipulations involving the Levi-Civita symbol

$$\begin{aligned}
&= 1/6\varepsilon_{\gamma\mu\nu}\varepsilon^{\gamma\mu\nu}\Big({}^{*}U^{(p)}_{\gamma\mu}\partial_\nu(\rho_{(p)}) + {}^{*}U^{(p)}_{\mu\nu}\partial_\gamma(\rho_{(p)}) + {}^{*}U^{(p)}_{\nu\gamma}\partial_\mu(\rho_{(p)})\Big) \\
&= 1/6\varepsilon_{\gamma\mu\nu}\Big(\varepsilon^{\gamma\mu\nu} {}^{*}U^{(p)}_{\gamma\mu}\partial_\nu(\rho_{(p)}) + \varepsilon^{\gamma\mu\nu} {}^{*}U^{(p)}_{\mu\nu}\partial_\gamma(\rho_{(p)}) + \varepsilon^{\gamma\mu\nu} {}^{*}U^{(p)}_{\nu\gamma}\partial_\mu(\rho_{(p)})\Big) \\
&= 1/6\varepsilon_{\gamma\mu\nu}\Big(\varepsilon^{\gamma\mu\nu} + \varepsilon^{\mu\nu\gamma} + \varepsilon^{\nu\gamma\mu}\Big) {}^{*}U^{(p)}_{\gamma\mu}\partial_\nu(\rho_{(p)}) \\
&= 1/2\varepsilon_{\gamma\mu\nu}\varepsilon^{\gamma\mu\nu} {}^{*}U^{(p)}_{\gamma\mu}\partial_\nu(\rho_{(p)}) \\
&= {}^{*}U^{(p)}_{\gamma\mu}\partial_\nu(\rho_{(p)})
\end{aligned}$$

putting this substitution into the sum, and using the definition of ${}^{*}U_{\gamma\mu}$ in terms of U^ν, we obtain

$$0 = \sum_{p=1}^{m} \epsilon_{(p)} \ {}^{*}U^{(p)}_{\alpha\beta}\Big(\varepsilon_{\nu\gamma\mu}U^{\xi}_{(p)}\partial_\xi(\rho_{(p)})\Big),$$

substituting in the joint density j and moving constants out of the sum recovers (23).

where the constant of proportionality is chosen based on item 1 above and the density parameter ρ is absorbed by increasing n. It is important to recognize that (26) only corresponds to the Hilbert portion of the full general relativity action (2). Appropriate forms for matter actions or cosmological constants lead to additional terms. In practice, Regge calculus is often used in the context of vacuum spacetimes where the extra terms are identically zero, or cosmological systems where the matter has a high degree of symmetry [24].

The field equation is given by varying the action with respect to a side l_p of a bone

$$\frac{\delta S_{\text{Regge}}}{\delta l_p} = \frac{1}{\kappa}\sum_n \frac{\partial L_n}{\partial l_p}\epsilon_n + \frac{1}{\kappa}\sum_n L_n \frac{\partial \epsilon_n}{\partial l_p} = 0 \tag{27}$$

It is possible to show that the second term vanishes [12, 19], which is sometimes (e.g. [21, 25]) called the Schläfli identity, a sketch of Regge's proof is in the next subsection. The first term can be rewritten[4], but the exact form it takes may be dependent on the bones in question.

3.2.1 Sketch of the proof $\sum_n L_n \frac{\partial \epsilon_n}{\partial l_p} = 0$

Again, we follow Regge's presentation[12]. Consider an D dimensional simplex T_D whose interior flat space has a Cartesian coordinate system. Label the dimension $D-1$ boundary simplices of T_D as T^r_{D-1}, and label the common $D-2$ simplex where T^r_{D-1} and T^s_{D-1} meet as T^{rs}_{D-2}. Each T^r_{D-1} has a unit normal vector U^r_μ, and the angle between T^r_{D-1} and T^s_{D-1} at T^{rs}_{D-2} is $\cos(\theta_{rs}) = U^{r,\mu}U^s_\mu$.

An antisymmetric tensor built from the normal vectors

$$V^{rs}_{\mu\nu} = \frac{U^r_\mu U^s_\nu - U^r_\nu U^s_\mu}{\sin(\theta_{rs})} \tag{28}$$

obeys

$$\begin{aligned} V^{rs}_{\mu\nu}V^{rs,\mu\nu} &= \frac{U^r_\mu U^s_\nu U^{r,\mu}U^{s,\nu} - U^r_\mu U^s_\nu U^{r,\nu}U^{s,\mu} - U^r_\nu U^s_\mu U^{r,\mu}U^{s,\nu} + U^r_\nu U^s_\mu U^{r,\nu}U^{s,\mu}}{\sin(\theta_{rs})^2} \\ &= \frac{1-\cos(\theta_{rs})^2 - \cos(\theta_{rs})^2 + 1}{\sin(\theta_{rs})^2} = 2 \end{aligned} \tag{29}$$

If we choose the coordinate system such that $U^r_0 = 1, U^r_\beta = 0$, for $\beta, \alpha \neq 0$, then

$$V^{rs}_{00} = 0,\ V^r_{0\beta} = \frac{U^s_\beta}{\sin(\theta_{rs})},\ V^r_{\beta 0} = \frac{-U^s_\beta}{\sin(\theta_{rs})},\ V^{rs}_{\alpha\beta} = 0. \tag{30}$$

If the measure of the simplex T^{rs}_{D-2} is L_{rs} then

$$\sum_s L_{rs}V^{rs} = 0. \tag{31}$$

[4] For instance, Regge [12] mentions $\frac{\partial L_n}{\partial l_p} \Rightarrow \cot(\theta_{np})$. The dedicated Regge calculus tutorial paper [19] mentions a case where the bones are approximately uniform isosceles triangles and $\frac{1}{8\pi}\sum_n \frac{\partial L_n}{\partial l_p}\epsilon_n \to \frac{l}{32\pi}\sum_n \cot(\theta_{np}/2)\epsilon_n$. We find this can be derived by assuming fixed height h and base l_p. The bone area will be $1/2 l_p h$, taking the derivative with respect to l_p gives $1/2h$. We use the fact that for the unaltered triangle $h = l/2\cot(\theta_{lp}/2)$, then $\frac{\partial L_n}{\partial l_p} \to \frac{1}{4l}\cot(\theta_{lp}/2)$

Consider the variation

$$\delta(U^{r,\mu}U^s_\mu) = \delta U^{r,\mu}U^s_\mu + U^{r,\mu}\delta U^s_\mu = -\sin(\theta_{rs})\delta\theta_{rs} \tag{32}$$

and the contraction

$$V^{rs}_{\mu\nu}U^{r,\mu}\delta U^{r,\nu} = \frac{U^s_\nu\delta U^{r,\nu} - [U^r_\nu\delta U^{r,\nu}\cos(\theta_{rs})]}{\sin(\theta_{rs})} \tag{33}$$

The term in the square brackets is 0 because $[U^r_\nu\delta U^{r,\nu} = 1/2\delta(U^r_\nu U^{r,\nu}) = 1/2\delta(1) = 0$, so we can write

$$\delta\theta_{rs} = -\frac{\delta U^{r,\mu}U^s_\mu + U^{r,\mu}\delta U^s_\mu}{\sin(\theta_{rs})} = -V^{rs}_{\mu\nu}(U^{r,\mu}\delta U^{r,\nu} + U^{s,\nu}\delta U^{s,\mu}) = V^{rs}_{\nu\mu}(U^{r,\mu}\delta U^{r,\nu} + U^{s,\nu}\delta U^{s,\mu}) \tag{34}$$

However, the deficit angle will be $\epsilon_n = 2\pi - \sum_r\sum_s\theta_{rs}$, so $\delta\epsilon_n = -\sum_r\sum_s\delta\theta_{rs}$. Then

$$\sum_r\sum_s L_{rs}\delta\theta_{rs} = \sum_r\sum_s L_{rs}V^{rs}_{\mu\nu}(U^{r,\mu}\delta U^{r,\nu} + U^{s,\nu}\delta U^{s,\mu}) = 0 \tag{35}$$

because $\sum_s L_{rs}V^{rs} = 0$. Recall that rs labels the $D-2$ bones of an individual simplex, summing this 0 over all simplices gives 0 for the whole network.

It is noteworthy that we have analytically verified a version of the Schläfli identity for a single tetrahedron using the Cayley-Menger cofactors to characterize the angles, see Appendix A.

3.3 Weak field Regge action

Assume now that we have perturbations about an approximately flat space. The edge lengths become $l_p = l_{p,0} + \delta l_p$. The bone area becomes

$$L_n = L_{n,0} + \sum_p \frac{\partial L_{n,0}}{\partial l_p}\delta l_p + \sum_{p,q}\frac{1}{2}\frac{\partial^2 L_{n,0}}{\partial l_p\partial l_q}\delta l_p\delta l_q + O(\delta l^3) \tag{36}$$

and the deficit angles become

$$\epsilon_n = 0 + \sum_p \frac{\partial\epsilon_n}{\partial l_p}\delta l_p + \sum_{p,q}\frac{1}{2}\frac{\partial^2\epsilon_n}{\partial l_p\partial l_q}\delta l_p\delta l_q + O(\delta l^3), \tag{37}$$

where the zeroth order term being identically 0 is a consequence of the background space being flat. Our total action is then

$$\begin{aligned}\frac{1}{\kappa}\sum_n L_n\epsilon_n =& \frac{1}{\kappa}\sum_n\Bigg(0\cdot L_{n,0} + \\ &\sum_p\big(L_{n,0}\frac{\partial\epsilon_n}{\partial l_p} + 0\cdot\frac{\partial L_{n,0}}{\partial l_p}\big)\delta l_p + \\ &\sum_{p,q}\Big(\frac{1}{2}L_{n,0}\frac{\partial^2\epsilon_n}{\partial l_p\partial l_q} + 0\cdot\frac{\partial^2 L_{n,0}}{\partial l_p\partial l_q} + \frac{\partial L_{n,0}}{\partial l_p}\frac{\partial\epsilon_n}{\partial l_q}\Big)\delta l_p\delta l_q + O(\delta l^3)\end{aligned} \tag{38}$$

Notice that the zeroth order term (top line) has a factor of 0 and cancels. The first order term (middle line) cancels as well, the $\big(L_{n,0}\frac{\partial \epsilon_n}{\partial l_p}$ portion due to the Schläfli identity and the other portion from the explicit 0 factor, so the lowest order surviving terms are the second order terms from the bottom line

$$\frac{1}{\kappa}\sum_n L_n\epsilon_n = \frac{1}{\kappa}\sum_n\sum_{p,q}\Big(\frac{1}{2}L_{n,0}\frac{\partial^2\epsilon_n}{\partial l_p\partial l_q} + \frac{\partial L_{n,0}}{\partial l_p}\frac{\partial\epsilon_n}{\partial l_q}\Big)\delta l_p\delta l_q + O(\delta l^3). \tag{39}$$

However, notice that the by taking a derivative of the Schläfli identity $\sum_n L_n\frac{\partial\epsilon_n}{\partial l_q} = 0$, we get $\frac{\partial}{\partial l_p}(\sum_n L_n\frac{\partial\epsilon_n}{\partial l_q}) = \sum_n L_n\frac{\partial^2\epsilon_n}{\partial l_q\partial l_p} + \frac{\partial L_n}{\partial l_p}\frac{\partial\epsilon_n}{\partial l_q} = 0$. Using this, we can rewrite the bottom line of (39) to obtain

$$\frac{1}{\kappa}\sum_n L_n\epsilon_n = \frac{1}{\kappa}\sum_n\sum_{p,q}\Big(\frac{1}{2}\frac{\partial L_n}{\partial l_p}\frac{\partial\epsilon_n}{\partial l_q}\Big)\delta l_p\delta l_q + O(\delta l^3), \tag{40}$$

a similar formula for the second order Regge action has been presented in [26].

4 The Ledger as a Regge calculus substrate

As stated before, the canonical RS ledger is a graph isomorphic to $\mathbb{Z}^3$, equipped with a uniform edge length ℓ_0 and a *recognition potential* $\psi > 0$ assigned to each vertex (or, equivalently, to each top-dimensional cell) by a sheaf structure. The potential ψ undergoes discrete "tick based" updates, so treating time as an additional coordinate gives an effective $\mathbb{Z}\times\mathbb{Z}^3$ flavor. Matter particles are patterns on the ledger, rather than being localized to a node and "hopping".

In order for the ledger to be extended to be a suitable substrate for Regge calculus, it needs a few extensions.

The hypercubic "cells" must be filled with an appropriate flat (Euclidean or Minkowski) space. This is necessary for the loops, homotopy/holonomy deformations, and vector parallel transport to be well defined. To that end, we define a *flat-interior ledger* $(\mathcal{K}, \{g_\sigma\})$ where $\mathcal{K}$ is a complex (the combinatorial ledger) and $\{g_\sigma\}$ assigns to each cell σ either a Euclidean flat metric (signature $s = +1$) or a Minkowski flat metric (signature $s = -1$), subject to the constraint that when two cells σ, σ' share a codim-1 face f, the induced metrics on f from g_σ and $g_{\sigma'}$ agree such that the distances between any two points on f are the same from the standpoint of σ and σ'. This ensures the curvature is confined to the codim-2 skeleton in accordance with the Regge framework:

1. Any closed loop γ contained in a single simplex is in flat space, so the parallel transport of any frame around γ returns to itself.

2. Any closed loop crossing only codim-1 faces (no codim-2 hinges) also has trivial parallel transport.

Regge calculus is conventionally defined with simplices, not hypercubes. Regge mentions in the context of 2 dimensional manifold approximations that "there is no loss in generality in supposing that all faces of M are triangles". In the context of 2 dimensional approximations of smooth manifolds with flat polygonal cells, any polygonal cell that is not a triangle can be subdivided into triangles by adding edges, and no alteration of the deficit angles at vertices needs to be made. In general, we can consider

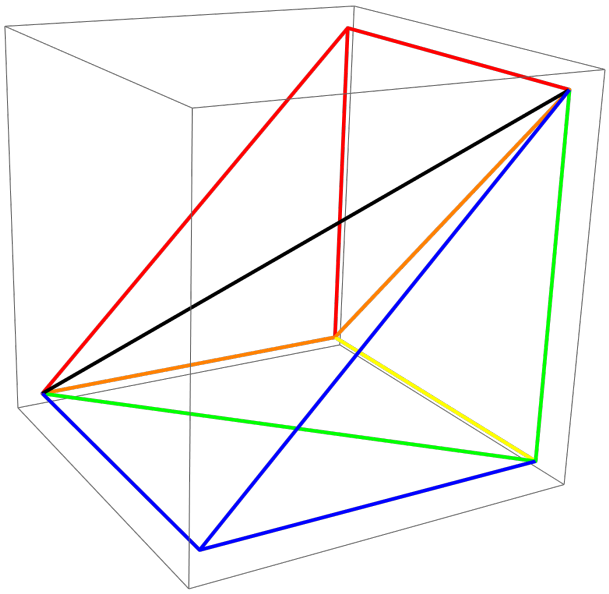

Figure 3: Illustration showing the Freudenthal triangulation of half of a cube. The red, yellow, and blue tetrahedrons all share the black edge, edges shared by yellow and blue are green and edges shared by yellow and red are orange. 3 congruent tetrahedrons fill half the cube, the full cube requires 6. Freudenthal triangulation of a 4D hypercube (as relevant to a ledger indexed by 3 spatial and 1 temporal dimension) would require 24 simplices.

adding additional divisions through the flat space cell σ interiors, or along the hypercube faces f, such that each hypercube is partitioned into simplices. For instance, a *Freudenthal triangulation* partitions an N dimensional hypercube into $N!$ congruent simplices (6 for the standard cube, 24 for a 4 dimensional hypercube) In the Freudenthal triangulation of a unit cube, the 6 tetrahedra share the body diagonal $(0,0,0),(1,1,1)$ as a common edge (the black edge in Figure 3.)

Because the additional dividers are partitioning flat space, they will have no associated deficit angle (or equivalently a full 2π sum of dihedral angles). Therefore,

$$S^{\text{simp}}_{\text{Regge}} = \underbrace{\sum_{h\in\text{cube}} L_h \epsilon_h}_{=S^{\text{cube}}_{\text{Regge}}} + \underbrace{\sum_{h\in\text{new}} L_h \cdot 0}_{=0} = S^{\text{cube}}_{\text{Regge}}. \tag{41}$$

The lengths must be allowed to vary In the Regge picture, the field equations are derived by varying side lengths, which cannot happen on a completely fixed lattice with constant ℓ_0 (or directly proportional to ℓ_0 times a fixed geometric factor for additional sides extending the hypercube lattice to a simplex mesh). One simple generalization is the "conformal edge length ansatz"

$$\ell_{ij} = \ell_0 \cdot \exp((\xi_i + \xi_j)/2) \tag{42}$$

which identifies a scalar log-potential on cells with an edge-length perturbation on the simplicial graph.

We discuss advantages and potential difficulties of this triangulated hypercube grid with interior flat space and deformable edge lengths according to the conformal edge ansatz as a Regge calculus substrate in Section 6.

4.1 Ledger cost

Consider a ledger (hypercube graph) with a *recognition potential* $\psi(\sigma_i) > 0$ assigned to each node by a sheaf structure and the following "cost"

Definition 4.1 (Global J-Cost)**.** *The total cost of the ledger configuration is*

$$\mathcal{J}_{global} = \sum_i \mathrm{J}\big(\psi(\sigma_i)\big) \cdot v_i + \sum_{\langle \sigma_i, \sigma_j \rangle} \mathrm{J}\left(\frac{\psi(\sigma_i)}{\psi(\sigma_j)}\right) \cdot w_{ij}, \tag{43}$$

where the first sum runs over all nodes and the second over edges, and v and w are node and edge weights

The first term penalizes local deviation from the cost minimum ($\psi = 1$). The second penalizes *mismatch* between neighbors. Define $\xi_i = \ln \psi(\sigma_i)$. Then:

$$\mathrm{J}\left(\frac{\psi_i}{\psi_j}\right) = \mathrm{J}(e^{\xi_i - \xi_j}) = \cosh(\xi_i - \xi_j) - 1 = \frac{(\xi_i - \xi_j)^2}{2} + O\big((\xi_i - \xi_j)^4\big)\,. \tag{44}$$

At leading order, the coupling cost is **quadratic** in the difference of log-potentials. This is the key structural fact that connects J-cost to the Regge action.

5 The Field-Curvature relationship

This section contains the central result of the paper: the connection of the linearized J-cost action with the linearized Regge action using the conformal edge ansatz.

5.1 The Regge action with the conformal edge length ansatz

Recall the Regge action (26), its extension to the nearly flat case (40), and the conformal edge length ansatz (42). Let the edges in question be such that edge p is between nodes i and j and edge q is between nodes k and l. From the conformal edge length ansatz,

$$\delta l_p = \ell_0 \cdot e^{(\xi_i + \xi_j)/2} - \ell_0 \approx \frac{\xi_i + \xi_j}{2} \ell_0, \tag{45}$$

with analogous expressions for δl_q in terms of k, l. Then

$$\frac{1}{\kappa} \sum_n L_n \epsilon_n \approx \frac{1}{\kappa} \sum_n \sum_{p=\langle i,j \rangle} \sum_{q=\langle k,l \rangle} \left(\frac{1}{2} \frac{\partial L_n}{\partial l_p} \frac{\partial \epsilon_n}{\partial l_q}\right) \frac{\ell_0^2}{4} (\xi_i + \xi_j)(\xi_k + \xi_l) \tag{46}$$

Notice that the factor in terms of the logarithmic field values expands to become a sum of products of individual pairs at vertices

$$(\xi_i + \xi_j)(\xi_k + \xi_l) = \xi_i \xi_k + \xi_i \xi_l + \xi_j \xi_k + \xi_j \xi_l. \tag{47}$$

Further, we can expand the sum over all $\sum_n \sum_{p=\langle i,j \rangle} \sum_{q=\langle k,l \rangle}$ and collect by vertex pairs $\langle a, b \rangle$, such that

$$\frac{1}{\kappa} \sum_n L_n \epsilon_n \approx \frac{1}{\kappa} \sum_{\langle a,b \rangle} M_{ab} \xi_a \xi_b \tag{48}$$

where M is some coefficient matrix.

5.1.1 Emergence of the Dirichlet form

If ij symmetry and zero row sum conditions on M have been established, we can apply the following lemma

Lemma 5.1 (Graph-Laplacian decomposition)**.** *Let $M : V \times V \to \mathbb{R}$ be symmetric with zero row sums: $M_{ij} = M_{ji}$ and $\sum_j M_{ij} = 0$ for every i. Then for any $\xi : V \to \mathbb{R}$,*

$$\sum_{i,j\in V} M_{ij}\,\xi_i\,\xi_j \;=\; -\frac{1}{2}\sum_{i,j\in V} M_{ij}\,(\xi_i-\xi_j)^2. \tag{49}$$

Proof. Expand $(\xi_i-\xi_j)^2 = \xi_i^2 - 2\,\xi_i\xi_j + \xi_j^2$. The ξ_i^2 piece is $\sum_{i,j} M_{ij}\,\xi_i^2 = \sum_i \xi_i^2 \sum_j M_{ij} = 0$ by the row-sum hypothesis; the ξ_j^2 piece is the same after swapping summation order and using symmetry. Hence $\sum_{i,j} M_{ij}(\xi_i-\xi_j)^2 = -2\sum_{i,j} M_{ij}\,\xi_i\xi_j$. □

If M has the correct symmetry and zero row sum properties, we can rewrite (48) as

$$S_{\text{Regge}} \approx -\frac{1}{2\kappa}\sum_{ij} M_{ij}(\xi_i-\xi_j)^2 \tag{50}$$

5.1.2 Reduction of the action: What has been proven

In the lean framework, a *weak-field Regge data* package consists of symmetric first-order responses

$$(\mathrm{d}A)_{ij}, \qquad (\mathrm{d}\delta)_{ij},$$

intended as the linearized hinge area and deficit angle for the edge between vertices i and j under the conformal ansatz (42). The second-variation coefficient matrix is the entrywise product

$$\tilde{M}_{ij} \;=\; (\mathrm{d}A)_{ij}\,(\mathrm{d}\delta)_{ij}. \tag{51}$$

The second-order Regge action is defined as

$$S^{(2)}[\xi] \;=\; \frac{1}{4}\sum_{i,j\in V} \tilde{M}_{ij}\,(\xi_i+\xi_j)^2. \tag{52}$$

Symmetry $\tilde{M}_{ij} = \tilde{M}_{ji}$ follows immediately from symmetry of the two factors (edges ij and ji are the same). In general, the zero row sum condition is currently discharged as a hypothesis `SchlaefliRowSum`: "$\forall i.\ \sum_j$ `bilinearCoefficient` $W\ i\ j$ `= 0`". However, for the special construction `laplacianReggeData A hA`, where the coefficient matrix is defined to be the graph Laplacian of a user-supplied symmetric edge-area A:

$$\texttt{dArea}_{ij} \equiv 1, \qquad \texttt{dDeficit}_{ij} = \delta_{ij}\sum_k A_{ik} - A_{ij}.$$

the zero row sum condition is a theorem (`schlaefliRowSum_laplacianReggeData`). Taking the form (52) with symmetry and row sums as GIVEN, then the proof of equivalence to the Dirichlet form is not a problem:

$$\begin{aligned} S^{(2)}[\xi] &= \frac{1}{4}\sum_{i,j\in V} \tilde{M}_{ij}\,(\xi_i+\xi_j)^2 \\ &= \frac{1}{4}\Big(\sum_{i,j\in V} \tilde{M}_{ij}\xi_i^2 + \sum_{i,j\in V} \tilde{M}_{ij}\xi_j^2 + 2\sum_{i,j\in V} \tilde{M}_{ij}\xi_i\xi_j\Big) \\ &= \frac{1}{2}\sum_{i,j\in V} \tilde{M}_{ij}\xi_i\xi_j. \end{aligned} \tag{53}$$

where the ξ^2 terms drop out due to the symmetry and row sum conditions, then we can use Lemma (5.1).

5.1.3 Reduction of the action: What has not been proven

Notice that there are similarities and differences between (46) and (52). The dependence on a product of first order variations in hinge size and deficit angle is the same. The Lean framework handles the constant factor κ separately, which is why it is not explicitly in the form of (52). The general second order variation (46) explicitly contains cross terms between different edges. While (52) does not, recall how in the derivation of that gathering by single vertex pairs leads to (48). Further, under the row sum and symmetry hypotheses, (53) shows that the $(\xi_i + \xi_j)^2$ and $\xi_i\xi_j$ terms are interchangeable up to a constant which could be absorbed into the definition of M vs $\tilde{M}$. There is no fully formalized calculation in the Lean framework deriving M or $\tilde{M}$ directly from the simplicial geometry for a concrete example. We describe some partial results, such as verification of the Schläfli identity for a tetrahedron, in Appendix A.

5.2 The Weak Field Identification

Explicitly putting (44) and (43) together, we obtain

$$\mathcal{J}_{\text{global}} \approx J_{\text{volume}} + \sum_{i,j} (\xi_i - \xi_j)^2/2 \cdot w_{ij}, \tag{54}$$

Notice the leading order mismatch term has the essentially the same structure that we managed to reduce from the linearized Regge action (50):

1. a double sum over i, j
2. a symmetric coefficient matrix, we have already explained the symmetry of M_{ij}, and the edge shared by σ_i and σ_j is the same as the edge shared by σ_j and σ_i (it is the same face)
3. The same dependence on $\frac{(\xi_i - \xi_j)^2}{2}$.

With some explicit differences:

1. In the Lean database, w_{ij} is treated as fixed edge weight data, whereas the exact form of M_{ij} is dependent, ultimately, on reducing the sums of all the $\left(\frac{1}{2}\frac{\partial L_n}{\partial l_p}\frac{\partial \epsilon_n}{\partial l_q}\right)\frac{\ell_0^2}{4}$ terms.
2. The Regge action has the Einstein coupling constant κ.

A mention should also be made of the extra J_{volume} term from (54). In the standard picture, the Regge action itself only corresponds with the Hilbert term from the full GR action (2), and additional terms are required for matter coupling. In terms of this simplified model, the J_{volume} could be considered as an effective treatment of a matter-like term, or possibly a cosmological constant like term if it is uniform.

$$\overbrace{J_{\text{volume}}}^{} + \underbrace{\sum_{i,j} \frac{(\xi_i - \xi_j)^2}{2} \cdot w_{ij}}^{} \text{ versus } \overbrace{S_{M,\Lambda,\ldots}}^{} + \underbrace{\sum_{i,j} (\frac{-M_{ij}}{\kappa}) \frac{(\xi_i - \xi_j)^2}{2}}^{}. \tag{55}$$

Even within the simplified model, this identification is only valid under the previously stated conditions of small ξ values/ weak field, the conformal edge map (42), the matrix symmetry and row sum conditions, etc.

5.2.1 Lean modules for formal verification

One of the distinctive aspects to the Recognition Science program is the focus on verifying results by formalizing them as theorems in the Lean 4 proof assistant [27]. Much of the argument presented in the current Section 4 here has been formalized with Lean and is available at `https://github.com/jonwashburn/shape-of-logic`. See Tables 1, 2 and 3 for lists of important files and information about their contents.

Table 1: Simplicial Ledger

File	Regge / piecewise-flat related content (summary)
IndisputableMonolith/Foundation/SimplicialLedger/	
`SimplicialLedger.lean`	Simplicial 3-complex ledger, recognition loops, 8-tick lower bound; geometric carrier used upstream of discrete gravity / Regge bridges (not hinge formulas here).
`ContinuumBridge.lean`	Definitional κ-normalized Laplacian bridge ($\kappa = 8\varphi^5$); discrete J-cost stationarity; continuum EFE not closed here; cites nonlinear Regge→EH via CMS.
`ContinuumTheorem.lean`	Phase D "field–curvature" certificate: composes cubic linearization discharge, κ_{Einstein} identification, unified `ContinuumFieldCurvatureCert`; explicitly *not* full nonlinear $O(a^2)$ Regge convergence.
`CubicDeficitDischarge.lean`	Cubic deficit functional and hinge list; leading quadratic truncation vs. full Cayley–Menger deficit; definitional discharge of `ReggeDeficitLinearizationHypothesis` on the cube.
`CubicSimplicialEquivalence.lean`	Cube vs. Freudenthal-type simplicial refinement: zero-deficit internal hinges, hinge-list additivity, `cubic_simplicial_action_equal` / refinement invariance of Regge-style sums.
`EdgeLengthFromPsi.lean`	Abstract hinge data, `DeficitAngleFunctional`, `regge_sum`; `ReggeDeficitLinearizationHypothesis`; field–curvature identity under that hypothesis; κ vs. `kappa_einstein`.
`InteriorFlat.lean`	Piecewise-flat "interior flat" simplices, trivial holonomy inside cells, curvature supported on codimension-2 hinges (Beltracchi §7).
`LorentzEmergence.lean`	Cubic lattice Laplacian dispersion vs. isotropic $\|k\|^2$ (continuum window); adjacent to continuum limit story, not hinge deficit definitions.
`NonlinearBridge.lean`	`NonlinearReggeJCostIdentity` hypothesis (full $\sum A_h \delta_h$ on conformal lengths); stationarity links; `NonlinearJCostReggeCert` (Beltracchi §6).
`SimplicialDeficitDischarge.lean`	Phase C5: general simplicial discharge of `ReggeDeficitLinearizationHypothesis`,via `CalibratedAgainstGraph` (pre-matched hinge/graph weights).

Table 2: Gravity

File	Regge / piecewise-flat related content (summary)
IndisputableMonolith/Gravity/	
`ReggeCalculus.lean`	Core scaffolding: `HingeData`, `deficit_angle`, `regge_action`, flat case, Regge equation variational scaffold, Gauss–Bonnet-style facts.
`DiscreteCurvature.lean`	Regge-style deficit angles on deformed cubic lattice, `curvature_from_deficit`, linearized Ricci from three-axis deficits, Gauss–Bonnet cube lemmas.
`DiscreteBianchi.lean`	Discrete Bianchi / loop constraints on deficit angles; imports `ReggeCalculus`; linearized vs. wrapped sums.
`LatticeRicci.lean`	Lattice Ricci from deficit curvatures; linearized equality exact at fixed d^2h; nonlinear Regge convergence stated as hypothesis `H_nonlinear_regge_convergence`.
`WeakFieldConformalRegge.lean`	Weak-field conformal reduction of Regge action; `WeakFieldReggeData`, Schläfli row-sum, `secondOrderReggeAction`, equivalence to discrete Dirichlet / `laplacian_action` at second order.
`NonlinearConvergence.lean`	Cheeger–Müller–Schrader-style axioms: Regge action / Ricci / holonomy errors $O(a^2)$ or $O(a^4)$; `RSReggeConvergence` certificate glue.
`NonlinearReggeProof.lean`	Narrative + `PhiLatticeRegularity` scaffold: which regimes are linearized vs. CMS-conditional; points to CMS for strong-field closure.

Table 3: Geometry

File	Regge / piecewise-flat related content (summary)
IndisputableMonolith/Geometry/	
`CayleyMenger*.lean`, `Cofactor*.lean`, `GramCayleyMenger.lean`	CM matrix, polynomial, cofactors, derivatives; realizability cone.
`DihedralCayleyMenger.lean`, `Dihedral*.lean`	$\cos\theta$ from cofactors; dihedral data and $\partial\theta/\partial L$.
`Schlaefli*.lean`, `DeficitLinearization.lean`	Schläfli interfaces; **proved** single-tet Shläfli; triangulation lift; deficit linearization.
`AffineIndepInterior.lean`, `TetrahedronRealization.lean`	Nondegenerate interior; Euclidean realization from edge lengths.
`ReggeTriangulation3D.lean`, `Triangulation3DConsistency.lean`, `ReggeRigorousFoundation.lean`	Finite 3D incidence; consistent edge lengths; conformal ansatz.
`ReggeHessian3D.lean`	Shared Hessian interface (`ReggeHessianData`).
`ReggeActionConcrete.lean`	Conformal Regge action; incidence Hessian; Dirichlet form.
`ReggeActionFirstVariation.lean`, `ReggeActionSecondVariation.lean`	First/second variation of nonlinear action; cubic remainder packaging.
`ReggeActionNonlinearHessianProof.lean`, `ReggeActionCubicTaylorBound.lean`, `ReggeActionNonlinearCorrespondence.lean`	Nonlinear Hessian chain rule; cubic Taylor bound; local Regge/J correspondence.
`Freudenthal*.lean`, `PeriodicFreudenthalTorus.lean`	Six-tet cube, strip, flat-sector demo; periodic torus model.
`ReggeClosureProgressAudit.lean`, `ReggeFullInterfaceAudit.lean`	Closure inventory; full interface status map.

6 Toward recovery of General Relativity from Regge calculus

Regge's original paper proposed the form of the action (26), but did not provide a rigorous characterization of the correspondence. Indeed, care needs to be taken when attempting to match Regge calculus systems to known exact general relativity solutions in practice, as different ways to quantify the error can seemingly lead to different qualitative behaviors [28, 29, 30]. However, Cheeger–Müller–Schrader provided a rigorous characterization of the convergence of piecewise-flat curvature measures to the smooth Lipschitz–Killing curvature measures under suitable fatness and smoothness hypotheses [31]. Translating their theorem into our notation gives

Theorem 6.1 (Cheeger–Müller–Schrader, 1984)**.** *Consider a smooth compact Riemannian manifold M with metric g. Denote a characteristic curvature length scale L_c, a smooth compact subspace of M as U with boundary ∂U, and the tubular neighborhood of width r around the boundary as $T_r(\partial U)$. For an approximation to the manifold made of sufficiently fat n dimensional simplices σ^n of maximum side length a, there exists some constant c such that*

$$\left| \sum_{h \in U} L_h \epsilon_h - \frac{1}{2} \int_U R\sqrt{g}\, d^n x \right| \leq c\left(\sqrt{\frac{a}{L_c}}\, Vol(U) + Vol(T_{\sqrt{aL_c}}(\partial U))\right), \tag{56}$$

where Vol is a generalized volume and h labels the $n-2$ dimensional hinges.

Considering a sequence of triangulations, the worst case bound on the convergence of the Regge action to the Einstein Hilbert action forced by Theorem 6.1 is effectively $O(a^{1/2})$. However, in numerical tests on approximating known solutions of general relativity, the observed convergence is frequently faster on regular lattices, with measured behavior of $O(a), O(a^2)$, and even $O(a^4)$ being observed in certain cases[28, 30].

Theorem 6.1 should be treated as a motivation rather than a strict proof for the emergence of the Einstein equations from general Regge calculus on triangulated manifolds. The primary reason is that they proved their result for Riemannian, rather than Lorentzian, manifolds. As mentioned before, Lorentzian manifolds present additional challenges in Regge calculus due to not having uniformly positive lengths. To our knowledge, no version of the theorem has been proven for Lorentzian manifolds. As a secondary point, theorem 6.1 is imported, there is not currently a version formally proved in the RS Lean database because the current Matlib lacks some of the necessary structures.

6.1 Advantages of the RS Cubic Lattice in a hypothetical GR recovery

On the RS lattice, we have

1. **Shape quality.** Freudenthal triangulation of hypercubes leads to identical simplices, and the simplices have a degree of "fatness", rather than being overly thin. The CMS theorem 6.1 required that the simplex fatness have a strict nonzero lower bound, which would be satisfied here unless the lattice were extremely deformed. Additionally, highly regular lattices frequently exhibit better convergence than the CMS bound.

2. **Natural UV cutoff.** The undeformed grid has native spacing ℓ_0. Disturbances on the grid will be bounded from below by its local resolution, which in the simplified model is dependent to the local average value of the logarithmic ξ field according to (42). If one were attempting to go beyond classical GR to use the Regge calculus as a starting point for quantum gravity as is sometimes done [26, 20], then a natural cutoff scale may be beneficial.

6.2 Possible difficulties with the RS Cubic Lattice

In the classical Regge calculus, the complex modeling the manifold is a tool, and different meshes for the same manifold may be equally valid. The ledger is intended to be a $\mathbb{Z}^3 \times \mathbb{Z}$ hypercubic lattice on which fields are defined and matter particles are patterns, so it needs to be treated as its own entity rather than merely a tool. This leads to certain difficulties:

1. **Manifold Cover** Approximating a manifold with simplices is nontrivial, which is one of the reasons Regge calculus has historically been less used in numerical relativity than other methods. Approximating a manifold with a triangulated hypercube lattice[5] as described here presents an additional difficulty: only the $D-2$ skeleton of the original hypercubes, not of the additional partitions for triangulation, can carry any deficit angle. This difficulty would be present in general augmented ledgers. A further difficulty is choosing how the deformation should be done. The conformal edge ansatz (42) used in the simplified model is restrictive. For instance, consider a single quadrilateral with corner potentials ξ_a, ξ_b, ξ_c, ξ_d, then the edge lengths are $\ell_{xy} = \ell_0 e^{(\xi_x+\xi_y)/2}$. It is possible to get larger or smaller squares and trapezoids, but it is not possible to get rectangles (one set of parallel edges longer than the other set of parallel edges). For certain sorts of geometries such as gravitational waves, it would in general be necessary to go beyond the conformal edge ansatz. However, it might be sufficient for standard cosmological solutions, which have vanishing Weyl tensor.

2. **Grid Effects and rotation invariance** Grids are fundamentally anisotropic at small scales. "Hopping" dynamics on grids recovers a taxicab geometry in the continuum limit, which is clearly unacceptable. However, pattern based dynamics can lead to the emergence of isotropic PDE terms such as the Laplacian in the continuum limit, so pattern based dynamics may be lead to acceptable behavior that reduces to rotation invariance when the length scales of variation are significantly above the lattice size.

3. **Preferred frame effects and boost invariance** If the ledger is an entity on which fields are defined, observers are ostensibly moving with respect to the ledger rest frame. It therefore needs to be explained how boost invariance arises, at least at length scales significantly above the lattice size.

It is noteworthy that in the recognition framework, there is a possible resolution to the preferred frame effects. Recognition geometry [17] examines discrete observables in an "event space" induced by finite resolution "recognizer" maps from an underlying

[5] *Locally* approximating a patch of a smooth manifold with a hypercubic lattice of the same dimension should always be possible, but *global* cover is not guaranteed.

configuration space. Suppose now the enhanced structure endowed with deformed edges, flat space cell interiors, and Freudenthal triangulation is an event space entity induced by recognition, rather than a state space entity. Then it is plausible that different observers create their own grid upon recognizing the configuration space.

While this solution might alleviate the boost invariance problem in some capacity, it raises its own questions about how the recognition process induces these properties, and how a grid orientation is assigned. Additionally, it does not address whether manifolds of physical interest can be approximated by a complex with curvature only on hypercube edges.

6.3 The strong field regime

Within the simplified model, we have shown in (55) that the linearized actions for the J cost and Regge actions take the same form, subject to the appropriate conditions outlined earlier. Linearized continuum GR recovers Newtonian gravity under appropriate assumptions (see Appendix B), typical lensing potentials, gravitational wave propagation at speed c, etc. Presumably linearized Regge calculus with appropriately fine grids would recover the same solutions[6], but the exact setup may be challenging. The structural identification (55) shows how $\mathcal{J}_{\text{global}}$ and the Regge calculus action can take the same form in the linearized regime. However, the derivation of (55) explicitly requires linearization on both the Regge and edge J terms. Thus, it does not demonstrate any correspondence beyond that regime. Whether a strong field correspondence between Regge calculus and the J cost can be formed, and under what sorts of additional conditions are required, is an open question.

7 Discussion

7.1 Connection to the ILG work

Previous recognition science work on gravity has been motivated by possible deviations from the continuum limit caused by the underlying discrete structure. Conceptually, the idea is that the underlying discrete limit of one event per tick creates an information processing lag, which manifests when the systems are sufficiently large. We give a brief description of the previously published work here. In C, we provide more details behind the mathematical framing, examine why changes to the original models are warranted, and provide speculation for future tests.

Mathematically, the original published hypothesis [32] was an enhancement of the effective density in the Newtonian Poisson equation

$$\nabla^2(\Phi) = 4\pi G\ \rho_{eff}, \tag{57}$$

where ρ_{eff} is written either in terms of a Riemann-Liouville integral

$$\rho_{eff}(t) = \rho(t) + C\tau_0^{-\alpha}\mathcal{I}^{\alpha}(\rho(t)), \tag{58}$$

or in terms of a spatial wavenumber

$$\rho_{eff}(k) \simeq \left(1 + C(\frac{k_0}{k})^{\alpha}\right)\rho(k) \tag{59}$$

[6]This adopts the common assumption that some generalization of the CMS convergence is true for 4D Lorentzian manifolds.

so that the effective k space Poisson equation is

$$-k^2\Phi(k) = 4\pi G\Big(1 + C(\frac{k_0}{k})^\alpha\Big)\rho(k). \tag{60}$$

The correction factor $\Big(1 + C(\frac{k_0}{k})^\alpha\Big)$ is given the symbol w, and the constants

$$\alpha = \frac{1}{2}\big(1 - \varphi^{-1}\big) \approx 0.191, \tag{61}$$

$$C = \varphi^{-2} \approx 0.382. \tag{62}$$

Because α is positive, the correction vanishes at high wavenumber, and an enhancement occurs at small wavenumber. For computational practicality, [32] fit a surrogate model

$$\frac{v(R)^2}{v_{baryon}(R)^2} = 1 + C\left(\frac{R}{r_0}\right)^\alpha, \tag{63}$$

where r_0 is the characteristic scale, to the SPARC dataset. The surrogate (63) performed better $\chi^2/N = 3.06$ than an analogous global fit of a ΛCDM galactic halo model $\chi^2/N = 5.27$, but not quite as well as MOND $\chi^2/N = 2.01$ [32].

The four conditions from B.1 for validity of the Newtonian Poission equation are widely considered to be met in galactic dynamics, the observed differences in behavior from Newtonian predictions being the motivation for considering modified gravity theories or dark matter. The current formulations of ILG treat deviations from Newtonian gravity at large scales (small spatial wavenumber), which is suitable for its purpose of galaxy modeling. Also, most present-day systems where strong-field effects are important (compact objects such as white dwarfs, neutron stars, and black holes) are much smaller than galactic scales, so ILG effects may be unimportant there. However, from a standpoint of theoretical cohesion, precision tests, or instances where assumption 1 of linearizeability from B.1 is met but at least one of the others is not, it would be desirable to determine the full behavior incorporating both the ILG effects and relativistic/ geometric effects from first principles.

7.2 Relation to Other Regge Calculus Approaches

Regge [12] formulated GR on simplicial complexes. Even within the classical regime, it is sometimes useful to use a $3+1$ split. The ledger, as an augmented grid with 3 spatial dimensions that evolves with 1 temporal dimension, naturally has this structure. There have been previous considerations of Regge calculus in the context of the $3+1$ split (see e.g. [33]). However, some of these programs cover the 3D spatial hypersurfaces with simplices and allow them to evolve in continuous time. The ledger structures naturally undergo "tick based" discrete time updates, so usage of a continuous time evolution is inappropriate for ledger based applications.

Loop quantum gravity. LQG quantizes holonomies and fluxes, producing discrete spectra for areas and volumes [34]. RS shares the emphasis on discrete structures but derives the lattice and its dynamics from a J cost based considerations.

Causal dynamical triangulations. Analogously to the common QFT path integral over allowed field configurations, CDT sums over allowed simplicial geometries [35]. RS fixes the lattice structure at the level of the hypercubes, although the refined triangulation does not enter the action directly and may be arbitrary.

8 Conclusion

Previous work in Recognition Science in the gravitational sector has focused on phenomenological modeling of galactic rotation curves, with ILG modifications to Newtonian gravity. However, the successes on general relativity mean that any serious program for fundamental gravitational physics should connect with it in some manner, for instance with gravity as a geometric effect, or possibly as a spin 2 field with universal coupling. In this paper, we show that extending the idea of the recognition science ledger, originally treated as a discrete graph on which dynamics were defined, to a cellular structure including deformable edge lengths and interior flat space, allowed for a substrate on which Regge calculus could be performed. Then, we showed the Regge action on the ledger, subject to the deformation (42), weak field linearization and the matrix symmetry and row sum conditions, reduces to a Dirichlet form on the node potentials. This Dirichlet form can be identified with an analogous linearization of the nearest neighbor J cost objective.

There are several avenues for future work. The theoretical framework of geometric gravity in Recognition Science still needs understanding of how to implement a richer variety of deformations, move beyond the weak field case, and explicit construction and machine verification of algorithms to compute the deficit angles and hinge sizes for triangulated hypercube lattices. Studying the behavior at small scales and implications on quantum gravity, and the emergence of the classical symmetries at scales much above the underlying cell size also needs consideration. On the phenomenological side, one avenue is additional ILG tests as described in C. Alternatively, attempting to formalize a framework with both ILG and relativistic effects would open up more sorts of tests such as lensing. Finally, it may be possible to further develop the general Regge calculus for Lorentzian manifolds and put the convergence bounds on a rigorous footing.

Acknowledgements: We would like to thank Milan Zlatanovic and Anil Thapa for helpful suggestions.
Author contributions: Conceptualization, J.W.; formal analysis, J.W. and P.B.; writing—original draft preparation, J.W.; writing—review and editing, J.W. and P.B.; figures, P.B.; Software, J.W. All authors have read and agreed to the published version of the manuscript.

A Geometry of tetrahedra

The *Cayley–Menger (CM) determinant* deals with the context of simplices. For a tetrahedron in Euclidean 3-space, it encodes volume: a non-degenerate simplex has

$$288\,V^2 = \mathrm{CM}_3(a), \tag{64}$$

where V is volume and a denotes the six squared edge lengths.

Label the vertices $0, 1, 2, 3$. Edges are indexed $e \in \{0, \ldots, 5\}$ with squared lengths

$$\begin{aligned} a_0 &= \ell_{01}^2 = L_0^2, & a_1 &= \ell_{02}^2 = L_1^2, & a_2 &= \ell_{03}^2 = L_2^2, \\ a_3 &= \ell_{12}^2 = L_3^2, & a_4 &= \ell_{13}^2 = L_4^2, & a_5 &= \ell_{23}^2 = L_5^2. \end{aligned}$$

Opposite pairs are $(0,5)$, $(1,4)$, $(2,3)$. The CM matrix for tetrahedra $M(a) \in \mathbb{R}^{5\times 5}$ has rows/columns $0,1,2,3,4$ with border of ones and vertex block filled by squared distances:

$$M(a) = \begin{pmatrix} 0 & 1 & 1 & 1 & 1 \\ 1 & 0 & a_0 & a_1 & a_2 \\ 1 & a_0 & 0 & a_3 & a_4 \\ 1 & a_1 & a_3 & 0 & a_5 \\ 1 & a_2 & a_4 & a_5 & 0 \end{pmatrix}. \tag{65}$$

As an explicit polynomial, the determinant is

$$\mathrm{cm3}(a) = 2\Big[a_0a_5\,(a_1+a_2+a_3+a_4-a_0-a_5) + a_1a_4\,(a_0+a_2+a_3+a_5-a_1-a_4) \tag{66}$$

$$+ a_2a_3\,(a_0+a_1+a_4+a_5-a_2-a_3) - a_0a_1a_3 - a_0a_2a_4 - a_1a_2a_5 - a_3a_4a_5\Big]. \tag{67}$$

Minors and cofactors $C_{r,c}$ of $M(a)$ enter the dihedral cosine formula

$$\cos\theta_n = \frac{C_{p,q}}{\sqrt{C_{p,p}\,C_{q,q}}}. \tag{68}$$

Explicitly, $C_{r,c} = (-1)^{r+c}\mathrm{Det}|M(\text{ drop row r, column c })|$. For instance, $C_{2,4} = a_0a_1 - a_0a_2 + a_0a_5 - a_1^2 + a_1a_2 + a_1a_3 - 2a_1a_4 + a_1a_5 + a_2a_3 - a_3a_5$ and $C_{1,1} = a_3^2 - 2a_3a_4 + a_4^2 - 2a_3a_5 - 2a_4a_5 + a_5^2$. Notice (68) is symmetric under exchange of p and q. Using our edge convention, the dihedral angle at a particular edge uses

$$\begin{aligned} &\theta_0 \to (p,q) = (4,3), \qquad &&\theta_1 \to (p,q) = (2,4), \qquad &&\theta_2 \to (p,q) = (2,3) \\ &\theta_3 \to (p,q) = (4,1), \qquad &&\theta_4 \to (p,q) = (3,1), \qquad &&\theta_5 \to (p,q) = (2,1) \end{aligned} \tag{69}$$

It is (68) that allows us to compute the Regge action for a complex of tetrahedra purely in terms of edge lengths that allows us to explicitly test the behavior of the Regge action.

A.1 The single tetrahedron Schläfli

Over a single tetrahedron, we have verified that

$$\sum_{n=0}^{5} \frac{\partial\theta_n}{\partial L_m} L_n = 0 \tag{70}$$

as a test for consistency in our formulas and numbering conventions, using both Wolfram Mathematica and inside the Lean framework (see `SchlaefliTetrahedronProof.lean` in the geometry folder). Notice that inside the Lean framework, the cofactors are written in terms of the squared edge lengths a_n so we need the chain rule factor $\frac{\partial f}{\partial L_n} = \frac{\partial f}{\partial a_n}\frac{\partial a_n}{\partial L_n} = 2\sqrt{a_n}\frac{\partial f}{\partial a_n}$.

A.2 A Freudenthal tetrahedron

As mentioned above, a Freudenthal triangulation divides a cube into 6 congruent tetrahedra. For concreteness,

$$L_0 = \sqrt{3}\ell, \quad L_1 = \ell, \quad L_2 = \sqrt{2}\ell, \quad L_3 = \sqrt{2}\ell, \quad L_4 = \ell, \quad L_5 = \ell \tag{71}$$

The associated dihedral angles are

$$\theta_0 = \pi/3, \quad \theta_1 = \pi/4, \quad \theta_2 = \pi/2, \quad \theta_3 = \pi/2, \quad \theta_4 = \pi/4, \quad \theta_5 = \pi/2 \tag{72}$$

It is possible to use the cosine formula (68) to determine $\frac{\partial \theta_x}{\partial L_y}$, which would show up in the Regge action. While the analytic formulas are lengthy, the values they take for this tetrahedron are

$$\frac{\partial \theta_{\text{row}}}{\partial L_{\text{column}}}|_{L_s \to \text{Eq (71)}} = \begin{pmatrix} 1 & 0 & -\sqrt{\frac{3}{2}} & -\sqrt{\frac{3}{2}} & 0 & \sqrt{3} \\ 0 & 0 & 0 & -\frac{1}{\sqrt{2}} & 1 & 0 \\ -\sqrt{\frac{3}{2}} & 0 & 1 & 2 & -\frac{1}{\sqrt{2}} & -\sqrt{2} \\ -\sqrt{\frac{3}{2}} & -\frac{1}{\sqrt{2}} & 2 & 1 & 0 & -\sqrt{2} \\ 0 & 1 & -\frac{1}{\sqrt{2}} & 0 & 0 & 0 \\ \sqrt{3} & 0 & -\sqrt{2} & -\sqrt{2} & 0 & 1 \end{pmatrix}. \tag{73}$$

The Schläfli terms are

$$L_{\text{row}} \frac{\partial \theta_{\text{row}}}{\partial L_{\text{column}}}|_{L_s \to \text{Eq (71)}} = \begin{pmatrix} \sqrt{3} & 0 & -\sqrt{3} & -\sqrt{3} & 0 & \sqrt{3} \\ 0 & 0 & 0 & -1 & 1 & 0 \\ -\frac{3}{\sqrt{2}} & 0 & \sqrt{2} & 2\sqrt{2} & -\frac{1}{\sqrt{2}} & -\sqrt{2} \\ -\frac{3}{\sqrt{2}} & -\frac{1}{\sqrt{2}} & 2\sqrt{2} & \sqrt{2} & 0 & -\sqrt{2} \\ 0 & 1 & -1 & 0 & 0 & 0 \\ 3 & 0 & -2 & -2 & 0 & 1 \end{pmatrix} \ell. \tag{74}$$

Notice that summing over any row here gives zero, as a consequence of the Schläfli identity.

B Standard Linearized General Relativity

The standard linearized version of general relativity is shown in many textbooks (e.g. [36, 1]), we include formulas and some minimal background here for completeness. The basic idea is that the metric can be written as

$$g_{\mu\nu} = \eta_{\mu\nu} + h_{\mu\nu} \tag{75}$$

where η is the Minkowski metric[7] and h is a perturbation. Keeping only terms of the first order in h, we obtain

$$g^{\mu\nu} = \eta^{\mu\nu} - h^{\mu\nu} \tag{76}$$

$$\Gamma^{\alpha}_{\mu\nu} = \frac{1}{2}\eta^{\alpha\beta}(\partial_\mu h_{\nu\beta} + \partial_\nu h_{\mu\beta} - \partial_\beta h_{\mu\nu}) \tag{77}$$

$$R_{\mu\nu\alpha\beta} = \frac{1}{2}(\partial_\alpha\partial_\nu h_{\mu\beta} + \partial_\beta\partial_\mu h_{\nu\alpha} - \partial_\beta\partial_\nu h_{\mu\alpha} - \partial_\alpha\partial_\mu h_{\nu\beta}) \tag{78}$$

$$R_{\nu\beta} = \frac{1}{2}\eta^{\delta\gamma}(\partial_\delta\partial_\nu h_{\gamma\beta} + \partial_\beta\partial_\delta h_{\nu\gamma} - \partial_\beta\partial_\nu h_{\gamma\delta} - \partial_\gamma\partial_\delta h_{\nu\beta}) \tag{79}$$

$$R = \partial_\alpha\partial_\beta h^{\alpha\beta} - \eta^{\alpha\beta}\partial_\alpha\partial_\beta h^{\gamma}_{\gamma} \tag{80}$$

$$G_{\mu\nu} = R_{\mu\nu} - \frac{1}{2}\eta_{\mu\nu}R \tag{81}$$

There are several difficulties inherent in examining perturbations in GR compared to other fields of physics. First, there is not a simple definition of "smallness" for the perturbation on a Lorentzian manifold[36]. Second, the diffeomorphism invariance leads to the possibility that the coordinate charts, rather than the underlying manifold, are what is being perturbed, which is typically dealt with by fixing gauge. Two different perturbations h and h' give the same linearized curvature tensor (and hence same physical content) if

$$h'_{\mu\nu} = h_{\mu\nu} + (\partial_\mu\xi_\nu + \partial_\nu\xi_\mu) \tag{82}$$

In the scalar-vector-tensor decomposition, the metric perturbations are broken into

$$h_{00} = -2\Phi \tag{83}$$

$$h_{0i} = w_i \tag{84}$$

$$h_{ij} = 2s_{ij} - 2\Psi\delta_{ij} \tag{85}$$

Here i ranges from 1 to 3 and s_{ij} is traceless. Under a change of gauge, the metric perturbations change as

$$\Phi' = \Phi - \partial_0\xi_0 \tag{86}$$

$$w'_i = w_i + \partial_0\xi_i - \partial_i\xi_0 \tag{87}$$

$$\Psi' = \Psi - \frac{1}{3}\sum_i \partial_i\xi_i \tag{88}$$

$$s'_{ij} = s_{ij} + \partial_i\xi_j + \partial_j\xi_i - (\frac{1}{3}\sum_i \partial_i\xi_i)\delta_{ij} \tag{89}$$

It is noteworthy that the dynamics of $h_{\mu\nu}$ on the background $\eta_{\mu\nu}$ are the same as those of a fundamentally spin 2 field on Minkowski space. Certain quantum gravity programs, particularly String Theory, conceptualize of gravity in terms of a spin 2 field with uniform coupling propagating on some fixed background.

[7]Similar first order perturbation schemes about different backgrounds, such as FLRW, are frequently considered

B.1 Emergence of the Poisson equation

A simple way to recover the Poisson equation is to move to the transverse gauge where $\partial_i s^{ij} = 0$ and $\partial_i w^i = 0$, then the Einstein tensor components become

$$G_{00} = 2\nabla^2\Psi \tag{90}$$

$$G_{0i} = -\frac{1}{2}\nabla^2 w_i + 2\partial_0\partial_i\Psi \tag{91}$$

$$G_{ij} = \delta_{ij}[\nabla^2(\Phi - \Psi) + 2\partial_0^2\Psi] - \frac{1}{2}\partial_0(\partial_i w_j + \partial_j w_i) - \partial^k\partial_k s_{ij} - \partial_i\partial_j(\Phi - \Psi) \tag{92}$$

If the source of the gravitational field is well approximated by "dust", $T_{\mu\nu} = \rho u^\mu u^\nu$ where u is a normalized 4 velocity, and time derivatives are negligible, then

$$2\nabla^2\Psi = \kappa\rho \tag{93}$$

$$-\frac{1}{2}\nabla^2 w_i = 0 \tag{94}$$

$$\delta_{ij}\nabla^2(\Phi - \Psi) - \nabla^2 s_{ij} - \partial_i\partial_j(\Phi - \Psi) = 0 \tag{95}$$

Because s_{ij} is defined to be traceless, taking the trace of (95) equation gives

$$2\nabla^2(\Phi - \Psi) = 0 \tag{96}$$

For the perturbations to vanish at infinity, $w_i = 0$ (more general forms compatible with $-\frac{1}{2}\nabla^2 w_i = 0$, such as a product of linear functions of each coordinate, grow without bound, and constants fail to vanish). By identical reasoning, (96) gives $\Phi - \Psi = 0$, from which equation (95) gives $\nabla^2 s_{ij} = 0 \implies s_{ij} = 0$.

To conclude, under the assumptions that

1. The metric perturbations are small enough that linearized GR is appropriate
2. The energy momentum tensor is dominated by the matter density term over stresses and momenta
3. The metric perturbations are quasi static such that time derivatives can be ignored
4. the metric perturbations vanish at infinity

Then we recover

$$\nabla^2\Phi = \frac{\kappa}{2}\rho \tag{97}$$

which is the Poisson equation for gravity.

The total metric in this case becomes

$$ds^2 = -(1 + 2\Phi)dt^2 + (1 - 2\Phi)(dx^2 + dy^2 + dz^2) \tag{98}$$

The geodesic equation

$$\frac{\partial^2 x^\mu}{\partial\tau^2} + \Gamma^\mu_{\alpha\beta}\frac{\partial x^\alpha}{\partial\tau}\frac{\partial x^\beta}{\partial\tau} = 0, \tag{99}$$

under the previous assumptions plus the condition for slow moving particles $\frac{dt}{d\tau} \approx 1$, $\frac{dx^i}{d\tau} << 1$ gives

$$\frac{d^2 x^i}{dt^2} = -\frac{\partial\Phi}{\partial x^i}. \tag{100}$$

While weak field perturbative general relativity recovers Newtonian gravity under the four assumptions listed above, it is important to remember that it is more general. Direct observations of deviation from Newtonian behavior within the solar system, gravitational wave propagation, frame dragging, Shapiro time delay, are all adequately explained by the linear theory. In many cases of empirical interest, lensing measurements can be described by the linear theory.

However, gravitational wave emission processes require going beyond the linearized theory in many cases, either because the fields are too strong (e.g. black hole mergers [37, 38, 39]), or the data is sufficiently good that small deviations from the linearized theory predictions can be measured (e.g. modern pulsar tests [40]). Black hole shadows [41, 42] or accretion [43, 44] also provide observational relevance of going past the linear approximation. Additionally to these empirical motivations, the linearized framework in metric perturbations $h_{\mu\nu}$ has problems with self consistency regarding the motivation for the geodesic equation [36].

C Information-Limited Gravity: Detailed analysis and essential modifications

In this appendix we provide analysis of the previous work on ILG, expose pathologies, and propose minimal modifications.

C.1 relation between published t and k forms of ρ_{eff}

Recall the equations relating the proposed form of the ILG enhancement in time (58) and k space (59). We show here how they are related. The Riemann-Liouville integral is

$$\mathcal{I}^{\alpha}(f(t)) = \frac{1}{\Gamma(\alpha)} \int_0^t (t-t')^{\alpha-1} f(t') dt' \tag{101}$$

Moving (58) to ω space with a Fourier transform[8], we obtain

$$\rho_{eff}(\omega) = \left(1 + C\tau_0^{-\alpha}(i\omega + 0^+)^{-\alpha}\right)\rho(\omega). \tag{102}$$

The authors of [32] propose a connection between finite propagation speed, spatial wavenumber, temporal frequency, and cosmological scale factor

$$\omega \simeq \frac{v_{max}\ k}{a}. \tag{103}$$

Using this substitution, and absorbing factors into k_0 gives (59).

C.2 Motivating the surrogate

While the authors of [32] do not elaborate on the reason for their choice, a plausible motivation for constructing the surrogate is as follows: For a spherical symmetric Newtonian

[8] The Riemann-Liouville integral is effectively a convolution of f with $g(t) = t^{\alpha-1}/\Gamma(\alpha)$, so its Fourier transform is the product of the Fourier transforms of f and g. The Fourier integral $\int_{-\infty}^{\infty} g(t)e^{-i\omega t}dt$ can be evaluated by using an $\omega \to \omega - i0^+$ regulator.

source,

$$a(R) = \frac{v(R)^2}{R} = \frac{G\int_0^R 4\pi r^2 \rho(r) dr}{R^2} \tag{104}$$

Assuming a uniform source, replacing ρ with ρ_{eff}, and using the fact that $k \propto 1/r$, we get

$$\frac{v(R)^2}{R} = \frac{G\int_0^R 4\pi r^2 \rho(1 + C(\frac{r}{r_0})^\alpha) dr}{R^2} \rightarrow \frac{4\pi G\rho(\frac{R^3}{3} + C\frac{R^{3+\alpha}}{(3+\alpha)r_0^\alpha})}{R^2}. \tag{105}$$

Dividing by the unenhanced case $4\pi G\rho R/3$ and absorbing the numeric factor $3/(3+\alpha)$ into a redefinition of the effective scale factor r_0 (which was the fit parameter), we recover (63)

C.3 Problems with the forms of (58) and (59)

It is noteworthy that (58) and (59) were phenomenological modeling choices rather than forms derived from first principles. While they (or at least the surrogate (63)) can be applied to galactic fits, they may not behave in other cases.

For instance, self-consistent application of the form of the k space kernel in (60) to cosmological perturbation theory will be problematic. Specifically, w diverges in the $k \rightarrow 0$ limit. Large scale perturbations will become arbitrarily strong. Further, the consistency of considering an unaltered homogeneous background, when any homogeneous contribution fed into w leads to a divergence, is dubious.

Another less obvious issue can be illustrated by applying (58) to a spherically symmetric mass distribution. Using the spherical form of the Laplacian gives

$$\frac{1}{r^2}\frac{\partial}{\partial r}(r^2\frac{\partial \Phi}{\partial r}) = 4\pi G(\rho(r,t) + \frac{C}{\tau_0^\alpha \Gamma(\alpha)}\int_0^t (t-t')^{\alpha-1}\rho(r,t')dt' \tag{106}$$

or

$$\frac{\partial \Phi}{\partial r} = \frac{G\int_0^r 4\pi r'^2 \rho(r',t)dr + \frac{C}{\tau_0^\alpha\Gamma(\alpha)}\int_0^r 4\pi r'^2 \int_0^t (t-t')^{\alpha-1}\rho(r',t')dt'dr'}{r^2} \tag{107}$$

Notice that $\int_0^r 4\pi r'^2\rho(r',t)dr = M(r,t)$ is simply the mass inside r at time t. If the function ρ is well behaved enough that the integration commutes,

$$\frac{\partial \Phi}{\partial r} = \frac{G\Big(M(r,t) + \frac{C}{\tau_0^\alpha\Gamma(\alpha)}\int_0^t (t-t')^{\alpha-1}M(r,t')dt'\Big)}{r^2} \tag{108}$$

Assuming the mass is conserved, for a location outside the mass distribution $M(r,t)$ is just a constant M. Then the integral in (108) can be done, resulting in

$$\frac{\partial \Phi}{\partial r} = \frac{GM\Big(1 + \frac{Ct^\alpha}{\alpha\tau_0^\alpha\Gamma(\alpha)}\Big)}{r^2} \tag{109}$$

which implies the acceleration of a test particle outside the mass distribution increases without bound as time goes on.

C.4 Possible modifications to the ILG kernels and future work

A minimal modification to the k space form of the ILG kernel that could be applied to cosmological perturbation theory in terms of comoving wavenumber is to impose an infrared cutoff $k_{\min} > 0$ such that the kernel only applies to sufficiently small perturbations:

$$w_{\text{pert}}(k_{\min}, k, a) = 1 + C\left(\frac{a}{c \max(k_{\min}, k)\, \tau_0}\right)^{\alpha}, \qquad w_{\text{bg}} = 1. \tag{110}$$

The Poisson equation for the cosmological perturbation theory then becomes

$$\nabla^2 \bar{\Phi} = 4\pi G\, \bar{\rho}, \qquad -k^2\, \delta\Phi(k, a) = 4\pi G\, w_{\text{pert}}(k_{\min}, k, a)\, \delta\rho(k, a). \tag{111}$$

A well motivated cutoff for cosmology is the inverse of the Hubble radius

$$k_{\min}(a) = \frac{a\, H(a)}{c}, \tag{112}$$

such that superhorizon modes are not enhanced. Notice that (111) formally fixes the problem with the divergences, is compatible with the galaxy results because the cutoff modification is well above galactic scales, and has been formalized in the Lean database in the files `IndisputableMonolith/ILG/Kernel.lean` and `IndisputableMonolith/ILG/PoissonKernel.lea` However, we do not consider any empirical tests regarding the rate of structure growth here, under which the kernel may not be successful. Computing the behavior of cosmological perturbation theory under (111) is a natural candidate for future work.

Away from the cosmological regime, using (103) to work backward from (59), we can motivate an enhancement of the form

$$w_{\text{dyn}}(T_{\text{dyn}}) = 1 + C\left(\frac{T_{\text{dyn}}}{\tau_0}\right)^{\alpha}. \tag{113}$$

Here T_{dyn} is the local orbital period (or, more generally, the inverse characteristic frequency of the system) and τ_0 is the characteristic time scale. Formally, this fixes the monotonic increase and divergence of the test particle acceleration. The disadvantage is a single T_{dyn} needs to characterize the system. While this is not a problem for periodic orbits, it would be difficult to assign a well motivated T_{dyn} to chaotic systems such as globular cluster dynamics.

One system that might be of relevance to studying (113) is the behavior of wide binaries. These have been a popular topic in dark matter consistency tests because in theory, dark matter would lead to no discernible alteration from Newtonian behavior in wide binary orbits, while MOND in general does[45]. Unfortunately, tests on GAIA data have only lead to confusion, with different papers preferring MOND [46, 47, 48] or Newtonian orbits [49, 50, 51], or in some cases conflicting with both [52]; It is likely [53, 54] that the various schemes used by different groups to control for low data quality and contamination by unresolved companions [55] lead to the different answers. Nevertheless, it may be possible to test wide binary orbits against the (113) in the future if data quality and companion detection improves.

References

[1] S.M. Carroll, *Spacetime and geometry: An introduction to general relativity* (2004).

[2] C.M. Will, *The Confrontation between General Relativity and Experiment*, *Living Reviews in Relativity* **17** (2014) 4 [1403.7377].

[3] N. Yunes, X. Siemens and K. Yagi, *Gravitational-wave tests of general relativity with ground-based detectors and pulsar-timing arrays*, *Living Reviews in Relativity* **28** (2025) 3 [2408.05240].

[4] E. Berti, E. Barausse, V. Cardoso, L. Gualtieri, P. Pani, U. Sperhake et al., *Testing general relativity with present and future astrophysical observations*, *Classical and Quantum Gravity* **32** (2015) 243001 [1501.07274].

[5] R. Penrose, *Gravitational collapse and space-time singularities*, *Phys. Rev. Lett.* **14** (1965) 57.

[6] S.W. Hawking and R. Penrose, *The Singularities of gravitational collapse and cosmology*, *Proc. Roy. Soc. Lond. A* **314** (1970) 529.

[7] A. Alzerkany, "Quantum gravity theory: Complete review with historical, theoretical, and problem-based perspectives." SSRN preprint, July, 2025. 10.2139/ssrn.5346400.

[8] C. Kiefer, *Quantum gravity – an unfinished revolution*, *arXiv e-prints* (2023) arXiv:2302.13047 [2302.13047].

[9] A. Barrau, *Testing different approaches to quantum gravity with cosmology: An overview*, *Comptes Rendus Physique* **18** (2017) 189 [1705.01597].

[10] J. Martin, *Everything you always wanted to know about the cosmological constant problem (but were afraid to ask)*, *Comptes Rendus Physique* **13** (2012) 566 [1205.3365].

[11] J. Washburn and M. Zlatanović, *Uniqueness of the canonical reciprocal cost*, *Mathematics* **14** (2026) .

[12] T. Regge, *GENERAL RELATIVITY WITHOUT COORDINATES*, *Nuovo Cim.* **19** (1961) 558.

[13] R.M. Williams and P.A. Tuckey, *Regge calculus: a brief review and bibliography*, *Classical and Quantum Gravity* **9** (1992) 1409.

[14] J.W. Barrett, D. Oriti and R.M. Williams, *Tullio Regge's legacy: Regge calculus and discrete gravity*, *arXiv e-prints* (2018) arXiv:1812.06193 [1812.06193].

[15] J. Washburn, M. Zlatanović and E. Allahyarov, *The d'alembert inevitability theorem*, *Mathematics* **14** (2026) .

[16] J. Washburn and A. Rahnamai Barghi, *Reciprocal convex costs for ratio matching: Axiomatic characterization*, *Axioms* **15** (2026) .

[17] J. Washburn, M. Zlatanović and E. Allahyarov, *Recognition geometry*, *Axioms* **15** (2026) .

[18] S. Pardo-Guerra, A. Thapa, M. Simons and J. Washburn, *Coherent comparison as information cost: Axiomatic foundations for discrete ledger dynamics*, *Foundations* **6** (2026) .

[19] R.R. Cuzinatto, C.A.M. de Melo and C. Naldoni de Souza, *Introduction to Regge Calculus for Gravitation*, *arXiv e-prints* (2019) arXiv:1904.01966 [1904.01966].

[20] R.M. Williams, *Discrete quantum gravity: The Regge calculus approach*, *Int. J. Mod. Phys. B* **6** (1992) 2097.

[21] B. Dittrich, L. Freidel and S. Speziale, *Linearized dynamics from the 4-simplex Regge action*, *Phys. Rev. D* **76** (2007) 104020 [0707.4513].

[22] R.D. Sorkin, *Lorentzian angles and trigonometry including lightlike vectors*, *arXiv e-prints* (2019) arXiv:1908.10022 [1908.10022].

[23] S.K. Asante, B. Dittrich and J. Padua-Argüelles, *Complex actions and causality violations: applications to lorentzian quantum cosmology*, *Classical and Quantum Gravity* **40** (2023) 105005.

[24] A.F. Jercher and S. Steinhaus, *Cosmology in Lorentzian Regge calculus: causality violations, massless scalar field and discrete dynamics*, *Classical and Quantum Gravity* **41** (2024) 105008 [2312.11639].

[25] A. Hedeman, H.M. Haggard, E. Kur and R.G. Littlejohn, *Symplectic and semiclassical aspects of the Schläfli identity*, *J. Phys. A* **48** (2015) 105203 [1409.7117].

[26] M. Rocek and R.M. Williams, *The Quantization of Regge Calculus*, *Z. Phys. C* **21** (1984) 371.

[27] L.d. Moura and S. Ullrich, *The Lean 4 Theorem Prover and Programming Language*, Springer-Verlag, Berlin, Heidelberg (2021), 10.1007/978-3-030-79876-5_37.

[28] M.A. Miller, *Regge calculus as a fourth-order method in numerical relativity*, *Classical and Quantum Gravity* **12** (1995) 3037 [gr-qc/9502044].

[29] L. Brewin, *Is the Regge Calculus a Consistent Approximation to General Relativity?*, *General Relativity and Gravitation* **32** (2000) 897 [gr-qc/9502043].

[30] L.C. Brewin and A.P. Gentle, *On the convergence of Regge calculus to general relativity*, *Classical and Quantum Gravity* **18** (2001) 517 [gr-qc/0006017].

[31] J. Cheeger, W. Muller and R. Schrader, *On the Curvature of Piecewise Flat Spaces*, *Commun. Math. Phys.* **92** (1984) 405.

[32] M. Simons, E. Allahyarov and J. Washburn, *A discrete informational framework for classical gravity: Ledger foundations and galaxy rotation curve constraints*, *Entropy* **28** (2026) .

[33] T. Piran and R.M. Williams, *Three-plus-one formulation of regge calculus*, *Phys. Rev. D* **33** (1986) 1622.

[34] C. Rovelli and F. Vidotto, *Covariant Loop Quantum Gravity: An Elementary Introduction to Quantum Gravity and Spinfoam Theory*, Cambridge University Press (2014).

[35] R. Loll, *Quantum gravity from causal dynamical triangulations: a review*, *Classical and Quantum Gravity* **37** (2020) 013002 [1905.08669].

[36] R.M. Wald, *General Relativity*, University of Chicago Press (1984).

[37] F. Pretorius, *Evolution of Binary Black-Hole Spacetimes*, *Phys. Rev. Lett.* **95** (2005) 121101 [gr-qc/0507014].

[38] B.P. Abbott, R. Abbott, T.D. Abbott, M.R. Abernathy, F. Acernese, K. Ackley et al., *Observation of Gravitational Waves from a Binary Black Hole Merger*, *Phys. Rev. Lett.* **116** (2016) 061102 [1602.03837].

[39] C. Cahillane and G. Mansell, *Review of the Advanced LIGO Gravitational Wave Observatories Leading to Observing Run Four*, *Galaxies* **10** (2022) 36 [2202.00847].

[40] M. Kramer, I.H. Stairs, R.N. Manchester, N. Wex, A.T. Deller, W.A. Coles et al., *Strong-Field Gravity Tests with the Double Pulsar*, *Physical Review X* **11** (2021) 041050 [2112.06795].

[41] T.E.H.T. Collaboration, K. Akiyama, A. Alberdi, W. Alef, K. Asada, R. Azulay et al., *First m87 event horizon telescope results. i. the shadow of the supermassive black hole*, *The Astrophysical Journal Letters* **875** (2019) L1.

[42] Event Horizon Telescope Collaboration, K. Akiyama, A. Alberdi, W. Alef, J.C. Algaba, R. Anantua et al., *First Sagittarius A* Event Horizon Telescope Results. VII. Polarization of the Ring*, *The Astrophysical Journal Letters* **964** (2024) L25.

[43] C.S. Reynolds, *Observational Constraints on Black Hole Spin*, *Annual Review Astronomy and Astrophysics* **59** (2021) 117 [2011.08948].

[44] C. Bambi, *Testing General Relativity with Black Hole X-Ray Data*, *Physics of Particles and Nuclei* **55** (2024) 1420 [2312.05857].

[45] X. Hernandez, M.A. Jiménez and C. Allen, *Wide binaries as a critical test of classical gravity*, *European Physical Journal C* **72** (2012) 1884 [1105.1873].

[46] X. Hernandez, *Internal kinematics of Gaia DR3 wide binaries: anomalous behaviour in the low acceleration regime*, *Monthly Notices of the Royal Astronomical Society* **525** (2023) 1401 [2304.07322].

[47] K.-H. Chae, *Breakdown of the Newton-Einstein Standard Gravity at Low Acceleration in Internal Dynamics of Wide Binary Stars*, *The Astrophysical Journal* **952** (2023) 128 [2305.04613].

[48] K.-H. Chae, *Measurements of the Low-acceleration Gravitational Anomaly from the Normalized Velocity Profile of Gaia Wide Binary Stars and Statistical Testing of Newtonian and Milgromian Theories*, *The Astrophysical Journal* **972** (2024) 186 [2402.05720].

[49] C. Pittordis and W. Sutherland, *Testing modified gravity with wide binaries in Gaia DR2*, *Monthly Notices of the Royal Astronomical Society* **488** (2019) 4740 [1905.09619].

[50] C. Pittordis and W. Sutherland, *Wide Binaries from GAIA EDR3: preference for GR over MOND?*, *The Open Journal of Astrophysics* **6** (2023) 4 [2205.02846].

[51] I. Banik, C. Pittordis, W. Sutherland, B. Famaey, R. Ibata, S. Mieske et al., *Strong constraints on the gravitational law from Gaia DR3 wide binaries*, *Monthly Notices of the Royal Astronomical Society* **527** (2024) 4573 [2311.03436].

[52] X. Hernandez, S. Cookson and R.A.M. Cortés, *Internal kinematics of Gaia eDR3 wide binaries*, *Monthly Notices of the Royal Astronomical Society* **509** (2022) 2304 [2107.14797].

[53] X. Hernandez, K.-H. Chae and A. Aguayo-Ortiz, *A critical review of recent Gaia wide binary gravity tests*, *Monthly Notices of the Royal Astronomical Society* **533** (2024) 729 [2312.03162].

[54] C. Pittordis, W. Sutherland and P. Shepherd, *Wide Binaries from GAIA DR3 : testing GR vs MOND with realistic triple modelling*, *The Open Journal of Astrophysics* **8** (2025) 109 [2504.07569].

[55] C.J. Clarke, *The distribution of relative proper motions of wide binaries in Gaia DR2: MOND or multiplicity?*, *Monthly Notices of the Royal Astronomical Society* **491** (2020) L72 [1910.10256].